Pharmaceutical Research, Vol. 11, No. 6, 1994

Research Article

The Role of Intramolecular Nucleophilic Catalysis and the Effects of Self-Association on the Deamidation of Human Insulin at Low pH

Richard T. Darrington[1,2] and Bradley D. Anderson[3,4]

Received July 9, 1993; accepted January 21, 1994

The influence of intramolecular catalysis and self-association on the kinetics of deamidation at the A-21 Asn residue of human insulin was explored at low pH and 35°C. Observed rate constants of overall insulin degradation were determined as a function of pH over a pH range of 2.0–5.0 and as a function of total insulin concentration between pH 2.0–4.0. The pH-rate behavior of both monomeric and associated insulin degradation from pH 2.0 to 5.0 indicated intramolecular catalysis by the unionized carboxyl terminus of the A chain. Anhydride trapping with aniline at pH 3.0 provided evidence supporting the formation of a cyclic anhydride intermediate in the rate limiting step indicative of intramolecular nucleophilic catalysis. Insulin in the presence of aniline at low pH formed two anilide products, A-21 $N^{\delta 2}$-phenyl asparagine and $N^{\delta 2}$-phenyl aspartic acid human insulin, at the expense of desamido A-21 formation, consistent with the partitioning of a common intermediate. Self-associated insulin degraded at a rate approximately 2.5 times greater than that of the monomer at pH 2.0 and pH 3. However, self-association had a negligible or slight stabilizing effect on insulin decomposition at pH 4.0. An apparent downward shift in the pK_a of the carboxyl terminus of approximately 0.75 units upon self-association and a catalytic rate constant which increases with -COOH acidity are proposed to account for these observations.

KEY WORDS: protein degradation; deamidation; human insulin; intramolecular catalysis, protein dimer formation; acyl transfer reactions.

INTRODUCTION

Nonenzymatic deamidation of Asn[5] and Gln residues, a major degradation pathway of proteins and peptides (1), involves amide side chain hydrolysis yielding a more acidic protein, often with altered *in vivo* activity (2–7). The inherent instability of Asn and Gln residues in proteins has led to the hypothesis that they serve as biological timers, regulating the development and aging of organisms (2,5,6). The kinetics of deamidation are highly dependent on factors such as temperature, ionic strength, pH and excipients (1,8), which has resulted in numerous complications during the synthesis, purification, characterization and formulation of proteins and peptides (1,2,9–19). Yet, comprehensive mechanistic studies of deamidation have been undertaken for only a limited number of proteins, and have been primarily confined to neutral and basic conditions (1,13,20).

Under non-acidic conditions deamidation of a number of internal Asn containing proteins has been shown to occur via intramolecular nucleophilic catalysis leading to the formation of a cyclic succinimide intermediate which can then undergo hydrolytic attack at either carbonyl resulting in a mixture of α or β linked Asp peptides (21,22). The existence of reactive cyclic intermediates may promote the formation of covalent dimers in protein formulations and delivery systems and, *in vivo*, may play a role in the immunogenicity of proteins (4,23–26). Under mildly acidic conditions, cyclic imide intermediates are apparently not involved in deamidation (8,27–29). However, Asp-X peptide bond scission, which becomes significant at low pH, may involve intramolecular catalysis, in this case by the Asp side chain carboxyl group (30). Intramolecular catalysis of Asp-X scission may involve general acid, the kinetically equivalent general base/specific acid, or intramolecular nucleophilic mechanisms (30–34). Recent attempts to characterize the mechanism of acid catalyzed peptide bond hydrolysis at Asp-X residues have been inconclusive (29).

At low pH, insulin undergoes preferential deamidation at the A-21 Asn, the carboxyl terminal residue of the A chain resulting in desamido A-21 insulin (DesA-21) (35). This reaction is most likely catalyzed intramolecularly by the pro-

[1] Present address: Glaxo Inc., Five Moore Drive, Research Triangle Park, North Carolina 27709.

[2] In partial fulfillment for a Ph.D. degree in the Department of Pharmaceutics and Pharmaceutical Chemistry, College of Pharmacy, University of Utah.

[3] Department of Pharmaceutics and Pharmaceutical Chemistry, University of Utah, Salt Lake City, Utah 84112.

[4] To whom correspondence should be addressed.

[5] Unless otherwise noted, all amino acids mentioned are the L-enantiomers of the 20 commonly occurring amino acids and are referred to by their three letter abbreviations.

0724-8741/94/0600-0784$07.00/0

tonated A-21 carboxyl terminus ($pK_a \approx 3.6$) and may serve as a model for acid catalyzed Asp-X peptide bond scission (31,32,36). Various mechanisms have been proposed including general acid (Scheme I(a)), general base/specific acid (Scheme I(b)), and nucleophilic catalysis (Scheme I(c)) (26,32,35,37). In this paper we have used the method of anhydride trapping with aniline to ascertain whether or not this reaction proceeds through a cyclic anhydride intermediate, indicative of intramolecular nucleophilic catalysis.

Quantitative, mechanistic studies of chemical reactions occurring in proteins are often complicated by a diverse array of self-associated species, each with their own characteristic reactivity, in equilibrium with the protein monomer in solution. Quantitative treatment of protein chemical reactivity therefore requires detailed knowledge of the self-association behavior, information which is typically unavailable.

The self-association of insulin, however, has been relatively well characterized in aqueous solutions. Insulin self-association consists of an equilibrium mixture of monomers, dimers, tetramers and hexamers, with the relative fraction of each species dependent on concentration, pH, and ionic composition (38–43). This study further examines the influence of self-association on deamidation at the A-21 Asn residue of human insulin at low pH.

MATERIALS AND METHODS

Unless otherwise noted all reagents were analytical grade and used as supplied. Chromatographic solvents were HPLC grade.

Reverse Phase High Performance Liquid Chromatography (RP-HPLC)

All kinetic studies and separations were carried out utilizing a modular RP-HPLC system consisting of two Beckman 110B pumps with mixer (Redmond, WA), a Beckman System Gold 406 analog interface, a NEC gradient controller (San Ramon, CA), a Rheodyne 7125 manual injector (Cotati, CA), and a Waters 740 data module and 441 UV detector with either a 214 or 254 nm filter (Milford, MA) or a dual monochromator fluorescence detector (Spectrovision Chelmsford, MA). Columns used, equipped with the appropriate guard, were as follows: Applied Biosystems (San Jose, CA) Brownlee Aquapore RP 300 C-8 (250×4.6 mm), (RP300); Brownlee spheri-5 C-18 (240×4.6 mm), (Spheri-5); Whatman (Hillsboro, OR) Partisil ODS-3 C-18 preparative (250×20 mm), (ODS-3); Rainin (Woburn, MA) Dynamax RP

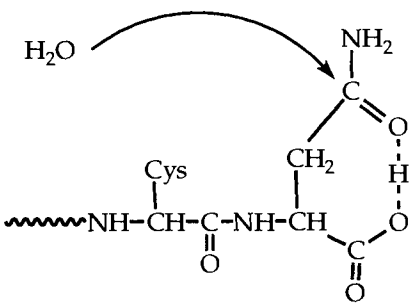

Scheme Ia. Intramolecular General Acid Catalysis.

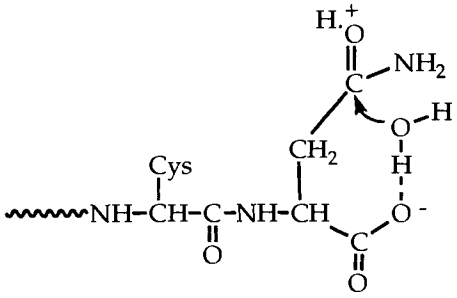

Scheme Ib. Intramolecular General Base/Specific Acid Catalysis.

300 C-8 semi-preparative (250×10 mm), (Dynamax). Specific columns used are noted in the appropriate section by their abbreviation. Elutions were performed using a mobile phase consisting of (A) 0.01M $(NH_4)_2SO_4$ adjusted to pH 2.0 with concentrated H_2SO_4 and (B) acetonitrile (Baxter Inc. Muskegon, MI) with 0.1% (v/v) trifluoroacetic acid, or (C) 95% 0.1M sodium phosphate pH 7.2, 4.5% methanol, 0.5% tetrahydrofuran and (D) methanol (Baxter Inc. Muskegon, MI). Mixtures or gradients of A and B, or C and D are listed in the appropriate sections.

Preparation of Zinc Free Human Insulin

Human insulin (recombinant DNA origin), commercially available as the parenteral formulation Humulin® R U-100 (Eli Lilly & Co., Indianapolis, IN), was converted into the zinc free neutral form by dialyzing 100 ml of Humulin R, adjusted to pH 2.0 with 1 M HCl, in 1000 MWCO tubing (Spectra/Por 6, Spectrum Medical Industries, Inc., Los Angeles, CA) against 5 L deionized H_2O at 4°C. Fresh deionized H_2O was cycled every 10 hours for a total of 7 cycles. The resulting zinc free insulin, containing less than 0.005 Zn atoms per hexamer as determined by plasma desorption spectroscopy (Perkin Elmer Plasma 40, Norwalk, CT), was lyophilized and the resulting amorphous solid was stored desiccated at 4°C. Purity by RP-HPLC was >99% with the major impurity being DesA-21.

Synthesis and Purification of DesA-21

DesA-21 was prepared from a 5 mg/ml solution of zinc free insulin in 0.1 M HCl which was adjusted to pH 2.0 by slowly adding 1M NaOH (to avoid excessive deviations in

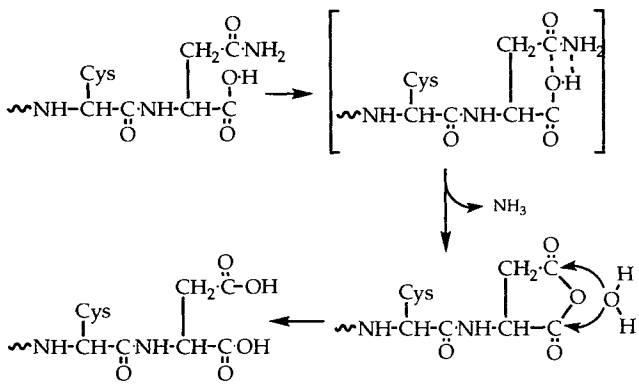

Scheme Ic. Intramolecular Nucleophilic Catalysis.

pH resulting in local precipitation) and placed in a 37°C oven (VWR Model #6000 San Francisco, CA). After 9 days approximately 65% of the native insulin had been converted to DesA-21 as determined by RP-HPLC. Purification was carried out by RP-HPLC using the ODS-3 column and a mobile phase gradient of 30% to 40% B at 0.33%/min at a flow rate of 4 ml/min with detection at 254 nm. The product peak was collected, dialyzed, and lyophilized using the previously mentioned procedures for zinc free human insulin. Characterization was achieved by RP-HPLC coelution with a reference sample of DesA-21 obtained from Eli Lilly & Co. Final purity was >99% by RP-HPLC with the major impurity being unmodified insulin.

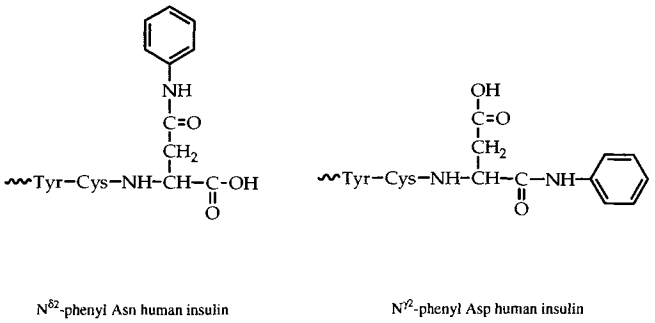

$N^{\delta 2}$-phenyl Asn human insulin $N^{\gamma 2}$-phenyl Asp human insulin

1. (Left) A-21 $N^{\delta 2}$-phenyl Asn derivative of human insulin. (Right) A-21 $N^{\gamma 2}$-phenyl Asp derivative of human insulin.

Preparation and Characterization of A-21 $N^{\delta 2}$-phenyl Asparagine and $N^{\gamma 2}$-phenyl Aspartic Acid Human Insulin

The anilides shown in Fig. 1 having a phenyl group affixed at either the $N^{\delta 2}$ of Asn or the $N^{\gamma 2}$ of Asp at the A-21 carboxyl terminus of insulin[6] were synthesized by adding 1.5 grams of aniline hydrochloride (Aldrich Milwaukee, WI) to 60 ml of Humulin R®. The resulting solution was adjusted to pH 4.0 with 1M HCl and stored at 37°C with stirring for 5 days, after which time approximately 40% of the native insulin had been converted to two new products, postulated to be aniline derivatives of insulin. Attempts to increase the fraction of chemically modified insulin resulted in the formation of significant amounts of unidentified side products. Chromatographic purification was performed using the Dynamax column and a mobile phase gradient of 27% to 50%B at 0.92%/min with a flow rate of 2.6 ml/min and UV detection at 254 nm. The resulting products, having retention volumes of 84.8 ml and 85.4 ml by RP-HPLC, were collected, dialyzed, and lyophilized as described previously for zinc free human insulin. Final purity of both products was >98% by RP-HPLC with the major impurities being native and DesA-21 human insulin.

Characterization of the chemically modified insulin was accomplished by enzymatic digestion using protease strain V8 type XVII-B isolated from Staphylococcus Aureus (P2922, Sigma St. Louis, MO) according to the method of Grau (44). Unmodified human insulin and an enzyme blank were included as controls. The V8 protease cleaves specifically at the C-terminal side of Glu residues; thus, insulin would be cleaved into four fragments, one of which should contain the modified residue. Separation of the fragments was accomplished by RP-HPLC using the RP300 column with an initial mobile phase of 84% A and 16% B. At 1 min. elapsed time the following gradient was initiated: 16% to 28.4%B at 0.7%/min, 28.4% to 50%B at 2.2%/min with a flow rate of 1.6 ml/min and UV detection at 214 nm. The fragments which contained the modified A-21 residue were identified by comparing the digestion patterns of modified and unmodified human insulin.

The modified fragments were collected and their molecular weights determined utilizing a Finnigan MAT 95 High Resolution GC/Mass Spectrometer (Bremen, Germany) supported by a Finnigan MAT ICIS II Operating System. The specific structure of each A-21 anilide insulin isomer was determined by digestion with Carboxypeptidase A (C6510, Sigma, St. Louis, MO) using the method of Slobin and Carpenter (45). Digestion solutions were monitored for the loss of starting material and appearance of modified material by RP-HPLC. The release of free amino acids was monitored using fluorescence detection by reacting the digestion mixture with o-phthaldialdehyde (OPA) (P-0657, Sigma) followed by RP-HPLC separation. The OPA stock solution (0.01M) was prepared by dissolving 0.067g OPA in 10 ml of MeOH followed by dilution to 50 ml with 0.25 M pH 9.5 borate buffer and kept at 4°C in the absence of light until use. Derivatizing solution was prepared immediately before use by adding 30 μl mercaptoethanol to 20 ml of the OPA stock solution. Derivatization of free amino groups was achieved by adding equal amounts of derivatizing solution and digestion mixture and vigorously vortexing for 30 seconds. The resulting mixture was then injected onto the Spheri-5 column after exactly 1 minute had elapsed. The initial mobile phase was 85% C and 15% D. At 5 min. elapsed time the following gradient was initiated: 15% to 35% D at 1.33%/min, 35% to 70% D at 1%/min, 70% to 80% D at 2%/min with a flow rate of 1 ml/min and fluorescence detection at 340 nm excitation and 455 nm emission.

Decomposition of Human Insulin under Mildly Acidic Conditions—Effect of pH and Concentration.

Observed rate constants of overall insulin decomposition (k_{obs}) were determined as a function of total insulin concentration at pH 2.0, 3.0 and 4.0, and under conditions where the monomer predominated (low [insulin]) at pH 2.0–5.0 (35°C, ionic strength, $\mu = 0.1$ (NaCl)) using the method of initial rates, allowing no more than 10% of the starting material to react. In some cases, these initial values were compared with first order rate constants obtained from the loss of insulin as a function of time over one half-life. Below pH 4.0 insulin reacted to form exclusively DesA-21, while above pH 4.0 at higher insulin concentrations some amide-linked dimer formation was noted. Hence, when applicable, k_{obs} was calculated from the sum of DesA-21 and amide linked dimer formation (46). Since the overall decomposition rate is governed by the rate of formation of the anhydride intermediate from which both products are produced (47), the effects of self-association on the overall rate reflect changes in the rate of intermediate anhydride formation.

[6] Based on IUPAC-IUB Commission on Biochemical Nomenclature. *J. Mol. Biol.* 52:1–17 (1970).

Appropriate amounts of insulin were added to dichlorodimethylsilane (DCDMS) treated volumetric flasks (to prevent adsorption of the predominantly positively charged molecule, pI = 5.4) and diluted to volume with the appropriate buffer (pH 2.0 HCl, pH 3.0 HCl or formate, pH ≥ 4.0 acetate). The resulting solutions (ranging from 2.67×10^{-7} to 9.36×10^{-4} M final insulin concentration) were then transferred to DCDMS treated glass vials in such a manner that there was a minimal air/water interface, sealed, and placed in a water bath at 35±0.1°C. Samples were removed at appropriate times, chilled and stored at 4°C. Insulin and DesA-21 insulin concentrations were determined by RP-HPLC using a RP-300 column and a mobile phase containing 72.3%A and 27.7%B at a flow rate of 1.2 ml/min with UV detection at 214 nm. When necessary, DesA-21 insulin and amide-linked dimer concentrations were concurrently determined utilizing the same RP-HPLC system with an initial mobile phase of 73%A and 27%B. At 1 min. elapsed time, the following mobile phase gradient was initiated: 27% to 29%B at 0.13%/min., 29% to 35%B at 0.6%/min. at a flow rate of 1.6 ml/min with UV detection at 214 nm.

DCDMS treatment of glassware was performed by treating the appropriate glassware with 15% (v/v) DCDMS/Toluene for 5 minutes at room temperature. The DCDMS/Toluene solution was then removed and the vials were rinsed repeatedly with toluene, MeOH, and deionized water followed by drying under a nitrogen gas stream.

Anilide Formation as a Function of Aniline Free Base Concentration at pH 3.0.

The initial rates of anilide formation were determined at 35°C as a function of aniline free base concentration ([AFB]) at pH 3.0 and μ = 0.1 (adjusted with NaCl). Insulin solutions (2×10^{-5} to 2×10^{-4} M) containing aniline ([AFB] = 1.4×10^{-5} to 6.2×10^{-3} M) were placed into DCDMS treated glass vials, tightly sealed with teflon/rubber septa screw caps and placed in a water bath at 35±0.1°C. Samples were removed at appropriate times, chilled and stored at 4°C. Insulin and A-21 anilide insulin concentrations were determined by RP-HPLC using a Dynamax column and an initial mobile phase of 73% A and 27% B. At 2 min. elapsed time the following gradient was initiated: 27% to 28% B at 0.4%/min, 28% to 35% B at 0.7%/min, 35% to 50% B at 1.5%/min at a flow rate of 2.6 ml/min and UV detection at 214 nm.

Data Analysis

Unless otherwise noted, all data were fit to the appropriate eqns. utilizing nonlinear least squares regression analysis software (MINSQ, MicroMath Inc, Salt Lake City, UT). Parameter uncertainties are reported as percent relative standard deviations (%rsd).

RESULTS

Insulin Degradation

pH-Rate Behavior

First order rate constants (k_{obs}) obtained by monitoring disappearance of insulin were identical to the initial rate constants of DesA-21 formation at pH 2.0, 3.0 and 4.0 under conditions which favor the monomer (low [insulin]). At pH values above 4.0 some amide-linked dimer formation was observed (46). In this case k_{obs} was calculated from the sum of $k_{DesA\text{-}21}$ and k_{dimer}. The addition of aniline had no significant effect on the observed rate of insulin loss. The pH-rate profile for insulin degradation from the monomer (solid curve) is shown in Fig. 2. The solid curve is based on the best fit of the data using Eqn. 1 with k_{cat}(monomer) = 1.92×10^{-3} hr^{-1} (6.97%rsd) and pK_a(monomer) = 4.06 (1.23%rsd). The enhanced reactivity of insulin when the A-21 terminal carboxyl group is unionized and the excellent fit of the data by Eqn. 1 is consistent with intramolecular catalysis of insulin degradation by the unionized terminal carboxyl group.

$$k_{obs} = k_{cat}\left(\frac{[H]^+}{K_a + [H]^+}\right) \quad (1)$$

k_{cat} may include contributions from general (k_{gen}) and nucleophilic (k_{nuc}) catalysis as illustrated in Eqn. 2; however, their relative contributions cannot be determined based solely on the pH-rate data.

$$k_{cat} = k_{gen} + k_{nuc} \quad (2)$$

The percent of total Asp released during digestion of DesA-21 with Carboxypeptidase A, which requires an L-α terminal carboxyl group, rapidly approached 100% indicating that racemization at the α carbon did not occur in the deamidation process.

Characterization of Anilides

In the presence of aniline at pH 3.0 deamidation of in-

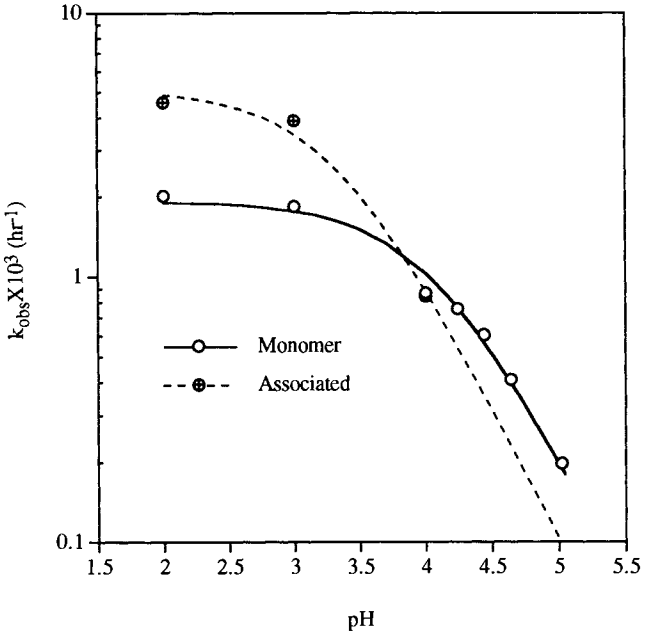

2. Comparison of the pH-rate profiles of human insulin degradation at 35°C from the monomer (solid curve) and the self-associated dimer (dashed curve). A shift in pKa of approximately 0.75 units is sufficient to account for the diminished reactivity of the associated dimer at higher pH.

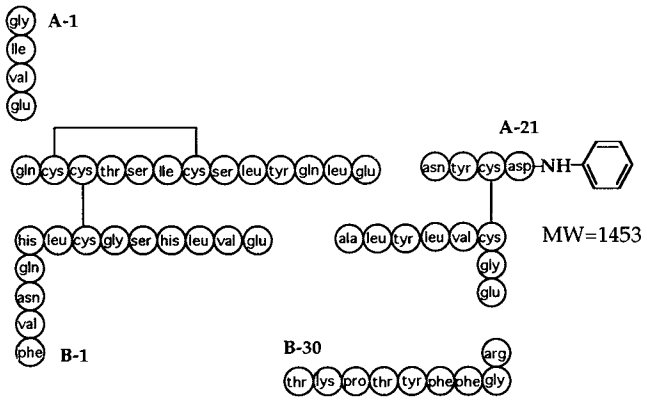

3. Expected Staphylococcus Aureus protease V8 cleavage pattern of A-21 N-phenyl human insulin. The mono isotopic molecular weight (MW) of the modified fragment is 1453.

sulin was in apparent competition with aniline attack, leading to the formation of two products with similar retention volumes (84.8 ml and 85.4 ml) by RP-HPLC. These products, postulated to be A-21 $N^{\delta 2}$-phenyl Asn and $N^{\gamma 2}$-phenyl Asp human insulin, were digested with protease V8 which resulted in the formation of four fragments. Fig. 3 shows the expected V8 digestion cleavage pattern for A-21 $N^{\delta 2}$-phenyl Asn and $N^{\gamma 2}$-phenyl Asp human insulin and the primary mono-isotopic molecular weight for the modified fragments. Comparison of the RP-HPLC elution profiles of protease digests of unmodified human insulin, Fig. 4(a) and either anilide, Fig. 4(b) revealed a shift in the retention time of peak II indicating that this peak represented the modified fragment. The digest elution profile was identical for the two anilide products. Fast Atom Bombardment mass spectra (FAB) of the modified fragments gave primary monoisotopic peaks (MH+) for both anilide fragments at 1454 amu. Solutions of either a single anilide isomer or a mixture of the two anilide isomers were digested with Carboxypeptidase A, which requires an L-α carboxyl terminus, and the loss of product was monitored by RP-HPLC. Only the isomer with the later retention time was altered over the two hour duration of the study, and free amino acid analysis by OPA derivatization showed that the amino acid released from the isomer which was cleaved did not correspond to any of the 20 commonly occurring amino acids. These results indicate that the anilide with the greater retention volume is A-21 $N^{\delta 2}$-phenyl Asn human insulin.

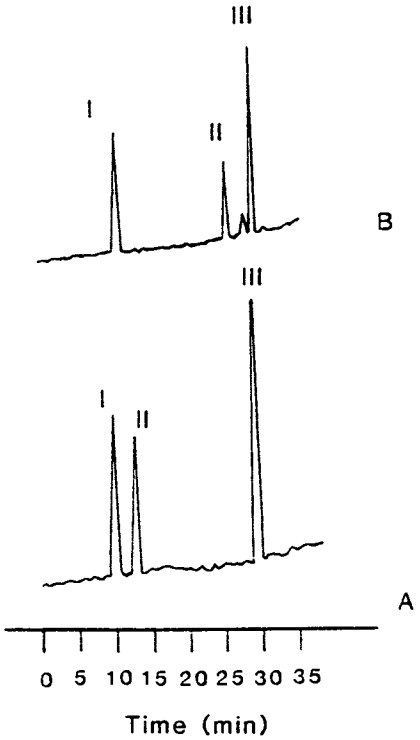

4(a). RP-HPLC elution profile of unmodified human insulin after cleavage by Staphylococcus Aureus protease V8. 4(b). RP-HPLC elution profile of A-21 N-phenyl human insulin after cleavage by Staphylococcus Aureus protease V8.

Anhydride Trapping with Aniline

The method of anhydride trapping with aniline is uniquely suited to delineate the relative contributions of k_{gen} and k_{nuc} to k_{cat} (48). A-21 $N^{\delta 2}$-phenyl Asn and $N^{\gamma 2}$-phenyl Asp form at the expense of DesA-21 in insulin solutions containing aniline at pH 3.0. There was no detectable lag time in the appearance of either anilide product. Fig. 5 illustrates the effect of [AFB] on (d[anilide]/dt)/[insulin] at pH 3.0 and $\mu = 0.1$. The curve represents a best fit of the data assuming that insulin in solutions containing aniline can react via the pathways shown in Scheme II. Based on the potential kinetic pathways illustrated in Scheme II, the rate of cyclic anhydride formation, (d[anhydride]/dt), can be expressed by Eqn. 3.

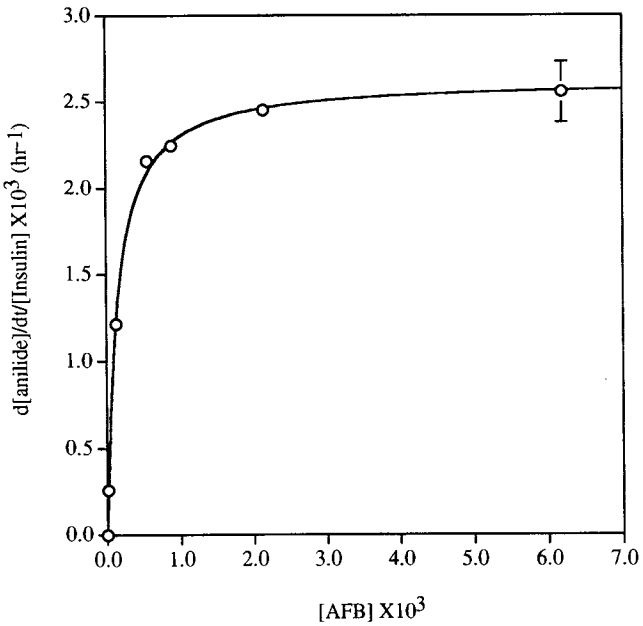

5. The effect of aniline free base concentration ([AFB]) on the observed rate of total N-phenyl Human Insulin formation (k_{obs}) where k_{obs} = (d[anilide]/dt)/[insulin]. The curve represents a nonlinear best fit of the data using Eqn. 6. The error bar represents the standard deviation of the data at constant [AFB] and an insulin concentration range of 2.6×10^{-5} to 2.5×10^{-4} M, (n = 3).

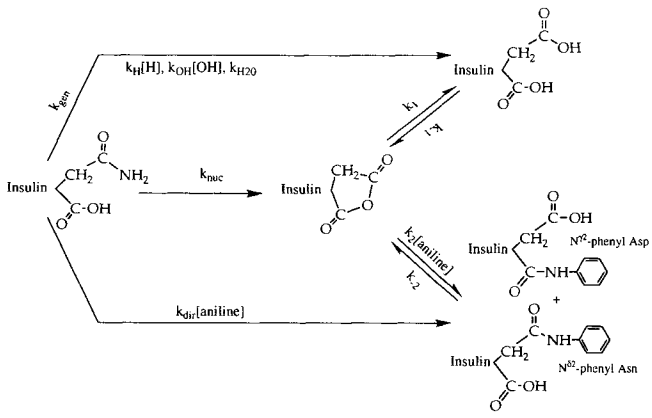

Scheme II.

$$\frac{d[\text{anhydride}]}{dt} = k_{nuc}[\text{insulin}] - [\text{anhydride}](k_1 + k_2[\text{AFB}]) + k_{-1}[\text{DesA} - 21] + k_{-2}[\text{anilide}] \quad (3)$$

Assuming the anhydride concentration is relatively small and rapidly reaches steady state then Eqn. 3 can be described by Eqn. 4 and the concentration of anhydride at steady state, ($[\text{anhydride}]_{ss}$), can be expressed by Eqn. 5.

$$\frac{d[\text{anhydride}]_{ss}}{dt} = 0 \quad (4)$$

$$[\text{anhydride}]_{ss} = \frac{k_{nuc}[\text{insulin}] + k_{-1}[\text{DesA} - 21] + k_{-2}[\text{anilide}]}{k_1 + k_2[\text{AFB}]} \quad (5)$$

The rate of anhydride formation from Des-A-21 insulin ($k_{-1}[\text{DesA} - 21]$) was found to be virtually zero and the maximum value for $k_{-2}[\text{Anilide}]$ was $2\times10^{-8}\text{Mhr}^{-1}$ under the conditions of this study. Thus, based on scheme II and Eqns. 3, 4 and 5 the rate of anilide formation can be described by Eqn. 6.

$$\frac{d[\text{anilide}]}{dt} = \frac{k_2k_{nuc}[\text{AFB}][\text{insulin}]}{k_1 + k_2[\text{AFB}]} + k_{dir}[\text{AFB}][\text{insulin}] \quad (6)$$

At high [AFB] when $k_2[\text{AFB}] \gg k_1$ Eqn. 6 reduces to

$$\frac{d[\text{anilide}]}{dt} = k_{nuc}[\text{insulin}] + k_{dir}[\text{AFB}][\text{insulin}] \quad (7)$$

As illustrated in Fig. 5, the overall rate of anilide formation increased with increasing [AFB] yet became independent of [AFB] at high [AFB]. The rate of anilide formation increased with increasing [AFB] and a concurrent decrease in DesA-21 formation which approached zero at high [AFB] was noted. The curve is based on Eqn. 6, where $k_{nuc} = 2.62\times10^{-3}\text{hr}^{-1}$ (6.2% rsd), $k_2/k_1 = 7.05\times10^{3}\text{M}^{-1}$ (5.6% rsd), and k_{dir} was not significantly different from zero. These observations indicate that k_{gen} does not contribute to k_{cat}, thus k_{cat} must be nucleophilic in nature (Eqn. 2). The effect of insulin concentration on the observed rate constants of anilide formation was minimal as demonstrated by the error bar in Fig. 5 which reflects the standard deviation of the observed rate constants of anilide formation at constant [AFB] with insulin concentrations ranging from 2.6×10^{-5} to 2.5×10^{-4} M (n = 3). The lack of an observed concentration effect is consistent with insulin being primarily in an aggregated state over this concentration range in the presence of aniline. The ratio of A-21 $N^{\delta2}$-phenyl Asn to $N^{\gamma2}$-phenyl Asp as determined by RP-HPLC was 2.69 and constant over the 50 fold range of [AFB] studied as illustrated in Fig. 6.

Influence of Self-Association on Human Insulin Decomposition at low pH.

The effect of total insulin concentration (Ct) on the rate constant governing the overall decomposition of human insulin (k_{obs}) at pH 2.0, 3.0 and 4.0 at 35°C and $\mu = 0.1$ (NaCl) is illustrated in Fig. 7. The curves represent best fits of the data using the following set of Eqns.

$$K_{12} = \frac{0.5(C_t - [\text{monomer}])}{[\text{monomer}]^2} \quad (8)$$

$$k_{obs} = k_{mon}f_{mon} + k_{dim}f_{dim} \quad (9)$$

$$f_{mon} = \frac{[\text{monomer}]}{C_t} \quad (10)$$

$$f_{dim} = \frac{2K_{12}[\text{monomer}]^2}{C_t} \quad (11)$$

$$C_t = [\text{monomer}] + 2K_{12}[\text{monomer}]^2 \quad (12)$$

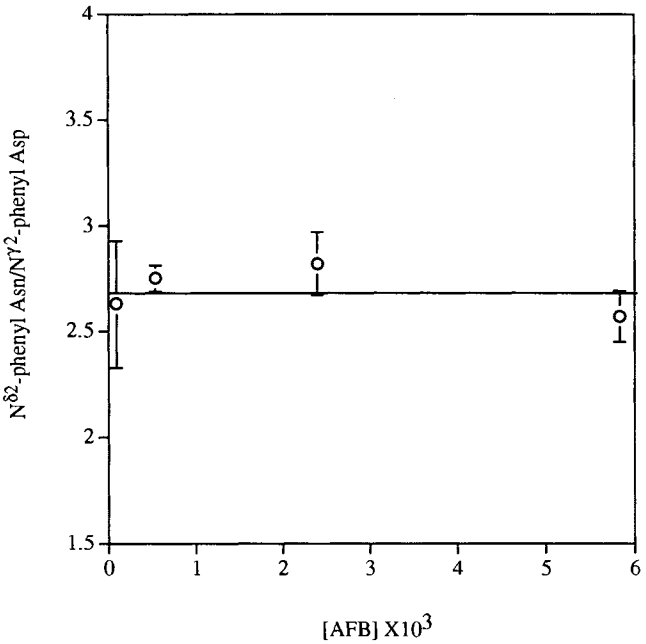

6. Product concentration ratio ($N^{\delta2}$-phenyl Asn/$N^{\gamma2}$-phenyl Asp) as a function of [AFB]. The error bars represent standard deviations due to variations in the product ratio as a function of time over the course of the initial rate kinetic study.

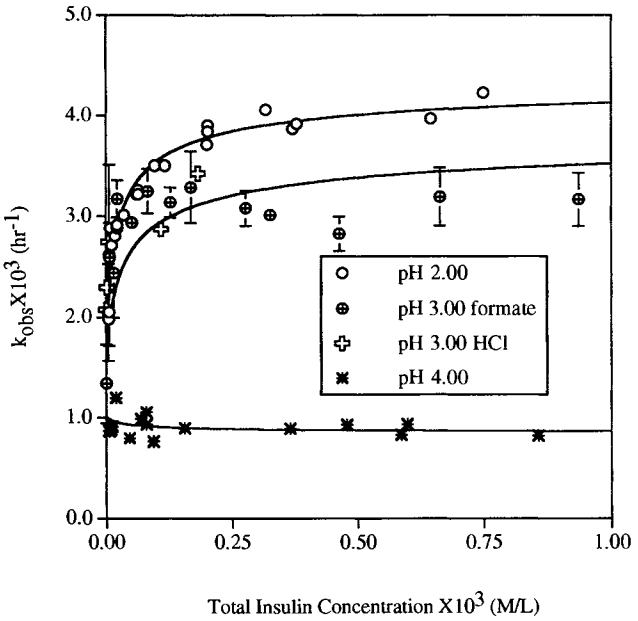

7. Psuedo first order rate constants for insulin degradation (kobs) as a function of total insulin concentration at 35°C and pH 2.0 (HCl), pH 3.0 (HCl and formate) and pH 4.0 (acetate). The curves are nonlinear regression fits of the data based on equations 8–12. Where applicable, error bars represent calculated standard deviations of the ordinate (n = 2).

where K_{12} is the monomer-dimer self-association equilibrium constant as determined by concentration difference spectroscopy (46), k_{mon} and k_{dim} are the micro deamidation rate constants for the monomer and dimer and f_{mon} and f_{dim} are the fractions of insulin existing as monomer and dimer in solution. The self-association model used assumes that only monomers and dimers exist at low pH, as proposed by Lord, et al. (40). The calculated values of k_{12}, k_{mon} and k_{dim} are noted in Table I. The pH-rate profile for insulin degradation from the associated dimer is shown in Fig. 2 (dashed curve). The dashed curve is based on the best fit of the data utilizing Eqn. 1 with $k_{cat}(\text{dimer}) = 5.12\times10^{-3}\text{hr}^{-1}$ (11.7%rsd) and $pK_a(\text{dimer}) = 3.31$ (6.04%rsd).

DISCUSSION

Evidence for the Formation of a Cyclic Anhydride Intermediate in the Deamidation of Human Insulin at Low pH.

Deamidation of the A-21 carboxyl terminal Asn is the primary degradation pathway of insulin below pH 4.0 (35,46,49). Leach and Lindley (50) reported that deamidation at carboxyl terminal Asn residues is intramolecularly catalyzed by the terminal carboxyl group at low pH. The results presented in this work support the hypothesis that deamidation of insulin at A-21 Asn involves intramolecular nucleophilic catalysis by the terminal carboxyl group resulting in the formation of a highly reactive cyclic anhydride intermediate as was first suggested by Slobin (35) and Carpenter (7) and refutes the mechanism involving intramolecular general acid or the kinetically equivalent general base/specific acid catalysis by the carboxyl terminus proposed by Markussen et al. (51).

Table I. Monomer and Dimer Deamidation Rate Constants and Monomer-Dimer Equilibrium Constants

pH	$k_m X10^3(hr^{-1})^{a,b}$	$k_d X10^3(hr^{-1})^{a,b}$	$K_{12}X10^{-4}(M^{-1})^{a,b}$
2.00	1.89 (0.01)	4.59 (0.01)	1.84 (0.25)
3.00	1.52 (0.14)	4.05 (0.35)	1.45 (0.23)
4.00	1.01 (0.06)	0.84 (0.05)	1.75 (0.40)

[a] Expressed as mean ± (standard deviation).
[b] Based on independent K_{12} determinations from concentration difference spectroscopy (46).

Evidence supporting A-21 Asn deamidation via catalysis by the terminal carboxyl group at low pH comes primarily from the pH-rate profile which deviates from the expected for specific acid catalyzed amide hydrolysis. Insulin degradation was virtually constant from pH 2 to 3 and decreased with increasing pH with a slope approaching −1 (Fig. 2) indicative of intramolecular catalysis by the protonated carboxyl terminus which may involve contributions from the kinetically equivalent pathways of general acid, general base/specific acid or nucleophilic catalysis by the A-21 terminal carboxyl group. The calculated pK_a(monomer) of 4.06 reported in this study is somewhat in disagreement with the previously reported value of 3.6 (36). However, the pK_a value presented in this study represents the actual pK_a value of the A-21 terminal Asn carboxyl group in the monomeric state while the previously reported value is actually an average of all titratable carboxylic groups in insulin with no distinction made between degree of association. A lower plateau in the pH-rate profile was not detected at pH values up to 5.02 suggesting that a kinetic contribution by the ionized carboxyl terminus (general base or nucleophilic catalysis by the ionized carboxyl group without acid catalysis) should be neglected.

In the presence of aniline, anilide derivatives are formed at both the α and β A-21 carbonyls with no apparent lag time in their formation, providing evidence that the intramolecular catalysis involves nucleophilic attack of the carboxyl group resulting in the formation of a cyclic anhydride intermediate. The distribution of $N^{\delta2}$-phenyl Asn and $N^{\gamma2}$-phenyl Asp noted in this study (2.7:1) is similar to the distribution of isoAsp versus Asp products which result from internal Asn deamidation of typical peptides (≈2.8:1) (8). Although deamidation of internal Asn residues and the subsequent formation of isoAsp and Asp containing proteins is the result of a cyclic imide rather than anhydride intermediate, these results are consistent with similar relative reactivities of the two carbonyl groups of the anhydride. The formation of anilide products proceeded with an accompanying decrease in DesA-21 formation as [AFB] increased with the rate of anilide formation approaching a constant value at high [AFB], consistent with partitioning of a common intermediate and indicating that only nucleophilic catalysis (k_{nuc}) is significant. The ratio of the rate constant governing anilide attack, and that governing attack by water (k_2/k_1) of $7.05\times10^3\ M^{-1}$ determined in this study is in excellent agreement with $k_{anilide}/k_{H2O}$ of $7.31\times10^3 M^{-1}$ for the cyclic anhydride of succinic acid as determined under similar conditions by Higu-

chi, et al. (52) providing further confirmation that a common cyclic anhydride intermediate is involved.

Anhydride trapping studies with aniline demonstrated that formation of the cyclic anhydride intermediate is rate determining. The plateau at high aniline free base concentrations (Fig. 5) suggests that direct attack by aniline does not occur in the rate determining step. Possibly this behavior could be attributed to a decrease in aniline reactivity due to aniline self-association, but Higuchi et al. (52) demonstrated that aniline reactivity does not decrease with increasing aniline concentration up to $[AFB] = 1 \times 10^{-2}$ M. At AFB concentrations below the plateau, the ratio of the two anilide products and the overall loss of insulin remained constant, providing evidence that intermediate formation is rate limiting even at low [AFB]. As [AFB] decreased ($k_2[AFB] \ll k_1$) water successfully competed with aniline for the anhydride intermediate; however, when aniline does react with the anhydride intermediate as governed by $k_2[AFB]$, the probability for its reacting with one carbonyl versus the other would be independent of [AFB], as expected if the formation of a common intermediate is rate limiting.

The observed rate constant for anilide formation at high [AFB] (Fig. 2) corresponds to the observed rate constant for deamidation at pH 3.0 in the absence of aniline (Fig. 7) which suggests that aniline does not influence the rate of cyclic anhydride formation.

Geiger and Clarke (8) reported that internal Asn deamidation could lead to racemization at the α carbon due to a lowering of the methine pK_a upon cyclization to an imide intermediate. Although racemization is also possible in a cyclic anhydride intermediate, the low pH and low steady state concentration of the intermediate in aqueous solutions may minimize this reaction. The fact that the A-21 Asp residue of DesA-21 insulin was completely cleaved by Carboxypeptidase A, which requires an L-α carbon containing carboxyl terminus as a substrate, indicates that racemization of L to D at the α carbon did not occur (53,54).

Reactive intermediates resulting from intramolecular nucleophilic catalysis play an important role in protein degradation and, *in vivo*, may play a role in the immunogenicity of proteins. Protein bond scission, deamidation, and amide-linked dimer formation often involve "hot spots" where cyclic anhydride or imide intermediate formation is favored, or where anchimeric assistance by spatially proximal catalytic residues can occur (55,56).

Reactive anhydride intermediates formed via intramolecular nucleophilic attack at the backbone carbonyl by Asp side chain carboxyls may be involved in Asp-X bond scission at low pH, explaining the rapid release of Asp in proteins under mildly acidic conditions (30,31,34,57). Recent studies of peptide bond scission at Asp-Gly linkages by Oliyai and Borchardt (29) support a mechanism involving intramolecular catalysis by the Asp side chain carboxyl, but solvent isotope studies aimed at discerning between general acid/base or nucleophilic catalytic mechanisms were inconclusive. Reactive anhydride intermediates may also result from nucleophilic attack by carboxyl residues spatially proximal by way of primary, secondary, tertiary, or quaternary structure. Wright, for example, proposed that the deamidation of Asn^{103} in horse heart cytochrome *c* involves intramolecular nucleophilic catalysis by a neighboring Glu^{102} side chain (56).

The Role of Self-Association in the Decomposition of Human Insulin

Insulin self-association increases decomposition at pH 2.0 and 3.0 by approximately 2.5-fold whereas it has a negligible or perhaps a slight stabilizing effect at pH 4.0 (Fig. 7). A recent study of the self-association of human insulin by concentration difference spectroscopy over this pH range conducted in these laboratories revealed that (a) the self-association of insulin between pH 2 and 4 can be described adequately by a simple monomer-dimer association model as employed by Lord *et al.* (40) and (b) the dimer formation constant (K_{12}) is approximately constant over this pH range, as demonstrated in Table I. Computer fits of k_{obs} versus total insulin concentration (Fig. 7) using this association model, described in Eqn. 9, yielded individual rate constants for cyclic anhydride formation in both monomeric and dimeric insulin (k_m and k_d) as a function of pH. These values are listed in Table I and plotted versus pH in Fig. 2. The shift in the pH-rate profile for the self-associated dimer can be rationalized by a decrease in the pK_a of the A-21 terminal carboxyl group of 0.75 units upon self-association. An increase in reactivity within the self-associated dimer at low pH ($pH < pK_a$) coupled with a decrease in pK_a on dimerization suggests a linear free energy relationship between the rate constant for cyclic anhydride formation and the pK_a of the catalytic carboxylic acid group (i.e., reactivity increases with acidity).

Although the monomer-dimer association model using a K_{12} value determined spectroscopically described the pH 2 kinetic data very well (Fig. 7), the pH 3 kinetic data gave a somewhat poorer fit. The pH 3 data could have been a better fit using a larger K_{12} than that obtained spectroscopically, but K_{12} values from concentration difference spectroscopy were considered more reliable than those obtained kinetically due to the poorer precision of the k_{obs} data. The pH 3 results were similar in both formate buffer and dilute HCl, thus ruling out a pronounced buffer effect on self-association. Thus, the poorer fit of the pH 3 data to the monomer-dimer model cannot be explained at this time.

Previous studies have shown that rates of intramolecularly catalyzed hydrolysis of amides and esters can be drastically affected by changes in conformational rigidity of the molecule (58–60). The rates of formation of anhydride or imide intermediates in proteins might therefore be expected to be significantly amplified or attenuated by conformational changes accompanying self-association, depending on the nature of the conformational changes. Studies by several groups have demonstrated that only minor conformational changes occur in monomer subunits upon insulin self-association to the dimer (61–64). Thus, the observed minor effects of self-association on insulin deamidation, reflecting a change in activation free energy of only 0.5 kcal/mol, are to be expected.

ACKNOWLEDGMENTS

The authors wish to acknowledge Dr. Ronald Chance

(Eli Lilly & Co.) for providing a reference sample of DesA-21 and Tim Dejulis for performing plasma desorption spectroscopy. FAB mass spectroscopy was performed by the University of Utah department of chemistry, funded by NSF #CH#-9002690 and the University of Utah Institutional Funds Committee. The remainder of the work described in this study was made possible by a Merck/INTERx predoctoral fellowship and a P.D.A. Foundation for Pharmaceutical Sciences, Inc. grant in biotechnology.

REFERENCES

1. A. B. Robinson and C. J. Rudd. Deamidation of Glutaminyl and Asparaginyl Residues in Peptides and Proteins. In B. L. Horecker and E. R. Stadtman (eds.), *Current Topics in Cellular Regulation*, Academic Press, New York, 1974, pp 247–295.
2. P. M. Yuan, J. M. Talent, and R. W. Gracy. Molecular Basis for the Accumulation of Acidic Isozymes of Triosephosphate Isomerase on Aging. *Mech. Aging Devel.* 17:151–162 (1981).
3. A. B. Robinson. Evolution and the Distribution of Glutaminyl and Asparaginyl Residues in Proteins. *Proc. Nat. Acad. Sci.* 71:885–888 (1974).
4. F. C. Westall. An Explanation for the Determination of "Self" Versus "Non-self" Proteins. *J. Theor. Biol.* 38:139–141 (1973).
5. A. B. Robinson, J. H. McKerrow, and P. Cary. Controlled Deamidation of Peptides and Proteins: An Experimental Hazard and a Possible Biological Timer. *Proc. Natl. Acad. Sci.* 66:753–757 (1970).
6. R. W. Gracy. Epigenetic Formation of Isozymes: The Effect of Aging. In M. C. Rattazzi, J. G. Scandalios and G. S. Witt (eds.), *Current Topics in Biological and Medical Research*, Alan R. Liss, Inc., New York, 1983, pp 187–201.
7. F. H. Carpenter. Relationship of Structure to Biological Activity of Insulin as Revealed by Degradative Studies. *Am. J. Med.* 40:750–758 (1966).
8. T. Geiger and S. Clarke. Deamidation, Isomerization, and Racemization at Asparaginyl and Aspartyl Residues in Peptides: Succinimide-Linked Reactions that Contribute to Protein Degradation. *J. Biol. Chem.* 262:785–794 (1987).
9. E. Sondheimer and R. W. Holley. Imides from Asparagine and Glutamine. *J. Am. Chem. Soc.* 76:2467–2470 (1954).
10. J. J. Sharp, A. B. Robinson, and M. D. Kamen. Synthesis of a Polypeptide with Lysozyme Activity. *J. Am. Chem. Soc.* 95:6097–6108 (1973).
11. C. Secchi, P. A. Biondi, A. Negri, R. Borroni, and S. Ronchi. Detection of Desamido Forms of Purified Bovine Growth Hormone. *Int. J. Peptide Protein Res.* 28:298–306 (1986).
12. U. J. Lewis and E. V. Cheever. Evidence for Two Types of Conversion Reactions for Prolactin and Growth Hormone. *J. Biol. Chem.* 240:247–252 (1965).
13. R. P. DiAugustine, B. W. Gibson, W. Aberth, M. Kelly, C. M. Ferrua, Y. Tomooka, C. F. Brown, and M. Walker. Evidence for Isoaspartyl (Deamidated) Forms of Mouse Epidermal Growth Factor. *Anal. Biochem.* 165:420–429 (1987).
14. R. L. Hill. Hydrolysis of Proteins. *Adv. Protein Chem.* 20:37–107 (1965).
15. G. F. Grannis. The Hydrolysis of Insulin and Human Serum Albumin in Dilute Hydrochloric Acid. *Arch. Biochem. Biophys.* 91:255–265 (1960).
16. T. J. Ahern and A. M. Klibanov. The Mechanism of Irreversible Enzyme Inactivation at 100°C. *Science.* 228:1280–1285 (1985).
17. H. Maeda and K. Kuromizu. Spontaneous Deamidation of a Protein Antibiotic, Neocarzinostatin, at Weakly Acidic pH. *J. Biochem.* 81:25–35 (1977).
18. C. G. Pitt. The Controlled Parenteral Delivery of Polypeptides and Proteins. *Int. J. Pharm.* 59:173–196 (1990).
19. M. J. Hageman, J. M. Bauer, P. L. Possert, and R. T. Darrington. Preformulation Studies Oriented toward Sustained Delivery of Recombinant Somatotropins. *J. Agric. Food Chem.* 40:348–355 (1992).
20. N. P. Bhatt, K. Patel, and R. T. Borchardt. Chemical Pathways of Peptide Degradation. I. Deamidation of Adrenocorticotropic Hormone. *Pharm. Res.* 7:593–599 (1990).
21. Y. C. Meinwald, E. R. Stimson, and H. A. Scheraga. Deamidation of the Asparaginyl-glycyl Sequence. *Int. J. Peptide Protein Res.* 28:79–84 (1986).
22. S. Clarke. Propensity for Spontaneous Succinimide Formation from Aspartyl and Asparaginyl Residues in Cellular Proteins. *Int. J. Peptide Protein Res.* 30:808–821 (1987).
23. H.-J. Helbig. *Insulindimerre aus der B-Komponente von Insulinpräparationen.* Dissertation. Rheinisch-Westfälischen Technischen Hochschule, Aachen. (1976).
24. D. C. Robbins and P. M. Mead. Free Covalent Aggregates of Therapeutic Insulin in Blood of Insulin-Dependent Diabetics. *Diabetes.* 36:147–151 (1987).
25. J. Brange, S. Havelund, and P. Hougaard. Chemical Stability of Insulin 2. Formation of Higher Molecular Weight Transformation Products During Storage of Pharmaceutical Preparations. *Pharm. Res.* 9:727–734 (1992).
26. J. Brange. Chemical Stability of Insulin 4. Mechanisms and Kinetics of Chemical Transformations in Pharmaceutical Formulations. *Acta Pharm. Nord.* 4:209–222 (1992).
27. K. Patel and R. T. Borchardt. Chemical Pathways of Peptide Degradation. II. Kinetics of Deamidation of an Asparaginyl Residue in a Model Hexapeptide. *Pharm. Res.* 7:703–711 (1990).
28. K. Patel and R. T. Borchardt. Deamidation of Asparaginyl Residues in Proteins: A Potential Pathway for Chemical Degradation of Proteins in Lyophilized Dosage Forms. *J. Parent. Sci. Tech.* 44:300–301 (1990).
29. C. Oliyai and R. T. Borchardt. Chemical Pathways of Peptide Degradation. IV. Pathways, Kinetics, and Mechanism of Degradation of an Aspartyl Residue in a Model Hexapeptide. *Pharm. Res.* 10:95–102 (1993).
30. S. Blackburn and G. R. Lee. The Liberation of Aspartic Acid during the Acid Hydrolysis of Proteins. *Biochem. J.* 58:227–231 (1954).
31. A. S. Inglis. Cleavage of Aspartic Acid. *Meth. Enzymol.* 91:324–332 (1983).
32. S. J. Leach. The Kinetics and Mechanism of Aspartic Acid Liberation From Proteins. Proceedings of the International Wool Textile Research Conference. C:C-181–198 (1955).
33. N. Kumar, D. Kella, W. E. Barbeau, and J. E. Kinsella. Effect of Disulfide Bond Cleavage on the Structure and Conformation of Glycinin. *Int. J. Peptide Protein Res.* 27:421–432 (1986).
34. J. Schultz, H. Allison, and M. Grice. Specificity of the Cleavage of Proteins by Dilute Acid. I. Release of Aspartic Acid from Insulin, Ribonuclease, and Glucagon. *Biochemistry* 1:694–698 (1962).
35. L. I. Slobin and F. H. Carpenter. The Labile Amide in Insulin: Preparation of Desalanine-Desamido-Insulin. *Biochemistry* 2:22–28 (1963).
36. C. Tanford and J. Epstein. The Physical Chemistry of Insulin. I. Hydrogen Ion Titration Curve of Zinc-free Insulin. *J. Am. Chem. Soc.* 76:2163–2176 (1954).
37. J. Markussen, I. Diers, P. Hougaard, L. Langkjaer, K. Norris, L. Snel, A. R. Sorensen, E. Sorensen, and H. O. Voigt. Soluble Prolonged-Acting Insulin Derivatives. III. Degree of Protraction, Crystallizability and Chemical Stability of Insulins Substituted in Positions A21, B13, B23, B27 and B30. *Prot. Engineer.* 2:157–166 (1988).
38. P. D. Jeffrey and J. H. Coates. An Equilibrium Ultracentrifuge Study of the Effect of Ionic Strength on the Self-Association of Bovine Insulin. *Biochemistry* 5:3821–3824 (1966).
39. P. D. Jeffrey and J. H. Coates. An Equilibrium Ultracentrifuge Study of the Self-Association of Bovine Insulin. *Biochemistry* 5:489–498 (1966).
40. R. S. Lord, F. Gubensek, and J. A. Rupley. Insulin Self-Association. Spectrum Changes and Thermodynamics. *Biochemistry* 12:4385–4391 (1973).
41. P. D. Jeffrey, B. K. Milthorpe, and L. W. Nichol. Polymerization Pattern of Insulin at pH 7.0. *Biochemistry* 15:4660–4665 (1976).
42. J. Goldman and F. H. Carpenter. Zinc Binding, Circular Dichroism, and Equilibrium Sedimentation Studies of Insulin (Bovine)

and Several of Its Derivatives. *Biochemistry* 13:4566–4574 (1974).
43. S. Strazza, R. Hunter, E. Walker, and D. W. Darnall. The Thermodynamics of Bovine and Porcine Insulin and Proinsulin Association Determined by Concentration Difference Spectroscopy. *Arch. Biochem. Biophys.* 238:30–42 (1985).
44. U. Grau. Fingerprint Analysis of Insulin and Proinsulins. *Diabetes*. 34:1174–1180 (1985).
45. L. I. Slobin and F. H. Carpenter. Action of Carboxypeptidase-A on Bovine Insulin: Preparation of Desalanine-Desasparagine-Insulin. *Biochemistry* 2:16–28 (1963).
46. R. T. Darrington and B. D. Anderson. The Effects of Concentration Dependent Self-Association and pH on the Deamidation and Covalent Dimerization of Human Insulin under Acidic Conditions. *In Preparation.*
47. Richard T. Darrington and Bradley D. Anderson. Concentration Dependence and the Role of Intramolecular Nucleophilic Catalysis in the Deamidation and Covalent Dimerization of Human Insulin at Low pH. *Pharm. Res.* 9S:S-228 (1992).
48. B. D. Anderson, R. A. Conradi, and W. J. Lambert. Carboxyl Group Catalysis of Acyl Transfer Reactions in Corticosteroid 17- and 21-Monoesters. *J. Pharm. Sci.* 73:604–611 (1984).
49. F. Sundby. Separation and Characterization of Acid-Induced Insulin Transformation Products by Paper Electrophoresis in 7 M Urea. *J. Biol. Chem.* 237:3406–3411 (1962).
50. S. J. Leach and H. Lindley. The Kinetics of the Amide Group in Proteins and Peptides. Part 2. Acid Hydrolysis of glycyl- and l-leucyl-l-asparagine. *Trans. Faraday Soc.* 49:921–925 (1953).
51. J. Markussen, U. Damgaard, K. H. Jorgensen, E. Sorensen, and L. Thim. Human Monocomponent Insulin. Chemistry and Characteristics. *Acta. Med. Scand., Suppl.* 671:99–105 (1983).
52. T. Higuchi, L. Eberson, and J. D. McRae. Acid Anhydride-Free Acid Equilibria in Water in Some Substituted Succinic Acid Systems and their Interaction with Aniline. *J. Am. Chem. Soc.* 89:3001–3004 (1966).
53. W. N. Lipscomb. Carboxypeptidase A. *Acc. Chem. Res.* 22:62–69 (1989).
54. R. P. Ambler. Carboxypeptidases A and B. *Meth. Enzymol.* 11:436–445 (1967).
55. H. T. Wright and A. B. Robinson. Cryptic Amidase Sites Catalyze Deamidation in Proteins. In N. O. Kaplan and A. Robinson (ed.), *From Cyclotrons to Cytochromes. Essays in Molecular Biology and Chemistry*, Academic Press, San Diego, 1982, pp 727–743.
56. H. T. Wright. Sequence and Structure Determinants of the Nonenzymatic Deamidation of Asparagine and Glutamine Residues in Proteins. *Protein Engineer.* 4:283–294 (1991).
57. B. Witkop. Nonenzymatic Methods for the Preferential and Selective Cleavage and Modification of Proteins. *Adv. Protein Chem.* 16:221–321 (1961).
58. T. C. Bruice and U. K. Pandit. The Effect of Geminal Substitution, Ring Size and Rotamer Distribution on the Intramolecular Nucleophilic Catalysis of the Hydrolysis of Monophenyl Esters of Dibasic Acids and the Solvolysis of the Intermediate Anhydrides. *J. Am. Chem. Soc.* 82:5858–5865 (1960).
59. T. C. Bruice and U. K. Pandit. Intramolecular Models Depicting the Kinetic Importance of "Fit" in Enzymatic Catalysis. *Proc. Natl. Acad. Sci. U.S.A.* 46:402–404 (1960).
60. T. Higuchi, L. Eberson, and A. K. Herd. The Intramolecular Facilitated Hydrolytic Rates of Methyl-Substituted Succinanilic Acids. *J. Am. Chem. Soc.* 88:3805–3808 (1966).
61. R. Palmieri, R. W. Lee, and M. F. Dunn. ^{1}H Fourier Transform NMR Studies of Insulin: Coordination of Ca^{2+} to the Glu(B13) Site Drives Hexamer Assembly and Induces a Conformation Change. *Biochemistry* 21:3387–3397 (1988).
62. M. Roy, R. W. K. Lee, J. Brange, and M. F. Dunn. ^{1}H NMR Spectrum of the Native Human Insulin Monomer: Evidence for Conformational Differences between the Monomer and Aggregated Forms. *J. Biol. Chem.* 265:5448–5452 (1990).
63. A. E. Mark, H. J. C. Berendesn, and W. F. V. Gunsteren. Conformational Flexibility of Aqueous Monomeric and Dimeric Insulin: A Molecular Dynamics Study. *Biochemistry* 30:10866–10872 (1991).
64. E. N. Baker, T. L. Blundell, J. F. Cutfield, S. M. Cutfield, E. J. Dodson, G. G. Dodson, D. M. C. Hodgkin, R. E. Hubbard, N. W. Isaacs, C. D. Reynolds, K. Sakabe, N. Sakabe, and N. M. Vijayan. The Structure of 2Zn Pig Insulin Crystals at 1.5 Å Resolution. *Philos. Trans. R. Soc. London B.* 319:369–456 (1988).